

Electroweak Multi-Higgs Production: A Smoking Gun for the Type-I Two-Higgs-Doublet Model

Tanmoy Mondal^{1,2,*}, Stefano Moretti^{3,4,†}, Shoaib Munir^{5,6,‡} and Prasenjit Sanyal^{7,§}

¹Department of Physics, Osaka University, Toyonaka, Osaka 560-0043, Japan

²Birla Institute of Technology and Science, Pilani, 333031, Rajasthan, India

³School of Physics and Astronomy, University of Southampton, Southampton SO17 1BJ, United Kingdom

⁴Department of Physics and Astronomy, Uppsala University, Box 516, SE-751 20 Uppsala, Sweden

⁵East African Institute for Fundamental Research (ICTP-EAIFR), University of Rwanda, Kigali, Rwanda

⁶Department of Physics, Faculty of Natural Sciences and Mathematics, St. Olaf College, Northfield, Minnesota 55057, USA

⁷Department of Physics, Konkuk University, Seoul 05029, Republic of Korea



(Received 26 April 2023; revised 6 October 2023; accepted 30 October 2023; published 5 December 2023)

Extending the Higgs sector of the standard model (SM) by just one additional Higgs doublet field leads to the two-Higgs-doublet model (2HDM). In the type-I Z_2 -symmetric limit of the 2HDM, all the five new physical Higgs states can be fairly light, $\mathcal{O}(100)$ GeV or less, without being in conflict with current data from the direct Higgs boson searches and the B -physics measurements. In this Letter, we establish that the new neutral as well as the charged Higgs bosons in this model can all be simultaneously observable in the multi- b final state. The statistical significance of the signature for each of these Higgs states, resulting from the electroweak (EW) production of their pairs, can exceed 5σ at the 13 TeV high-luminosity Large Hadron collider (HL-LHC). Since the parameter space configurations where this is achievable are precluded in the other, more extensively pursued, 2HDM types, an experimental validation of our findings would be a clear indication that the true underlying Higgs sector in nature is the type-I 2HDM.

DOI: [10.1103/PhysRevLett.131.231801](https://doi.org/10.1103/PhysRevLett.131.231801)

Introduction.—The existence of additional Higgs bosons, besides the one discovered by the LHC [1,2] (hereafter, denoted by H_{obs}), is predicted by most (if not all) frameworks of new physics. Observation of a second Higgs boson will thus provide firm evidence that the underlying manifestation of the EW symmetry breaking (EWSB) mechanism is a nonminimal one.

From a theoretical point of view, given the fact that the H_{obs} belongs to a complex doublet field in the SM, any additional Higgs field can be naturally expected to have the same $SU(2)_L$ representation. Following this argument, even the minimal bottom-up approach of augmenting the SM with a second doublet Higgs field and assuming CP -invariance yields a total of five physical Higgs states after EWSB: two neutral scalars (h and H , with $m_h < m_H$), one pseudoscalar (A), and a charged pair (H^\pm). If both the doublets Φ_1 and Φ_2 in this 2HDM couple to all the fermions of the SM, they would cause flavor-changing neutral currents (FCNCs) that contradict the experimental results. To prevent these FCNCs, a \mathbb{Z}_2 symmetry can be imposed [3,4], under which $\Phi_1 \rightarrow \Phi_1$, $\Phi_2 \rightarrow -\Phi_2$,

$u_R^i \rightarrow -u_R^i$, $d_R^i \rightarrow -d_R^i$, $e_R^i \rightarrow -e_R^i$, so that all the quarks and charged leptons (conventionally) couple only to the Φ_2 , resulting in the so-called type-I 2HDM (see Refs. [5,6] for detailed reviews).

By now, many studies [7–24] have established that the additional Higgs states (when the H_{obs} is identified with either the h or the H state) of the 2HDM can be individually accessed at the LHC. Therefore, several searches for singly produced neutral and charged Higgs bosons have been carried out by the ATLAS and CMS Collaborations (see, e.g., [25–32]), but they remain elusive thus far. Even if a single state is eventually observed, the corresponding measurements that will ensue will, however, not enable one to ascertain which of the many possible extended realizations of the Higgs mechanism is at work.

The majority of analyses, both phenomenological and experimental ones, involving an electrically neutral multi-Higgs final state, concentrate on QCD-induced production modes, namely, gluon fusion and $b\bar{b}$ annihilation. While such gluon-initiated production is evidently highly dominant in the SM, it is not necessarily so in new physics models, owing to the nonstandard couplings of their new Higgs bosons to the fermions and gauge bosons. In a previous analysis [33] it was shown that the inclusive cross sections for the $q\bar{q}^{(\prime)}$ -induced production, where q represents predominantly a u or d quark, of neutral multi-Higgs final states can be larger than their QCD-induced

Published by the American Physical Society under the terms of the [Creative Commons Attribution 4.0 International license](https://creativecommons.org/licenses/by/4.0/). Further distribution of this work must maintain attribution to the author(s) and the published article's title, journal citation, and DOI. Funded by SCOAP³.

production, over sizeable parameter space regions of the Type-I 2HDM with standard hierarchy ($H_{\text{obs}} \equiv h$). The charged final states can of course only be produced via EW processes.

In this Letter, through a complete detector-level Monte Carlo (MC) analysis, we concretely establish that EW production can provide simultaneously visible signals of all the three additional Higgs bosons of the type-I 2HDM at the LHC with 3000 fb^{-1} integrated luminosity. The model parameter space configurations where this is possible contain an A lighter than the H_{obs} , with the H and H^\pm not much heavier, and are therefore well motivated, in that the entire Higgs spectrum lies at the EW scale. Our signature channel, constituting of multiple b quarks, allows a full reconstruction of the H , A , and H^\pm masses. It implies that the LHC can uniquely pin down (or definitively rule out) the underlying EWSB mechanism as this (albeit narrow) parameter space region of the Type-I 2HDM (or at least as a low-energy manifestation of a grander framework with a Higgs sector mimicking this model). What makes our results all the more special is the fact that such a particular Higgs boson mass spectrum is forbidden in the Type-II 2HDM [34] (the realization aligning with minimal supersymmetry).

The Letter is organized as follows. In Sec. II we very briefly review the Type-I 2HDM and its parameter space configurations relevant for multi-Higgs production, and identify a benchmark point (BP) satisfying the most important theoretical and experimental constraints. In Sec. III we detail our MC analysis, and in Sec. IV we establish the potential of the LHC to extract all the Higgs boson masses in the model. We present our conclusions in Sec. V.

The Type-I 2HDM.—Higgs potential and parameters: The most general potential of a CP -conserving 2HDM can be written as

$$\begin{aligned} \mathcal{V} = & m_{11}^2 \Phi_1^\dagger \Phi_1 + m_{22}^2 \Phi_2^\dagger \Phi_2 - [m_{12}^2 \Phi_1^\dagger \Phi_2 + \text{H.c.}] \\ & + \frac{\lambda_1}{2} (\Phi_1^\dagger \Phi_1)^2 + \frac{\lambda_2}{2} (\Phi_2^\dagger \Phi_2)^2 + \lambda_3 (\Phi_1^\dagger \Phi_1)(\Phi_2^\dagger \Phi_2) \\ & + \lambda_4 (\Phi_1^\dagger \Phi_2)(\Phi_2^\dagger \Phi_1) + \left[\frac{\lambda_5}{2} (\Phi_1^\dagger \Phi_2)^2 + \text{H.c.} \right]. \end{aligned} \quad (1)$$

It is convenient to write the doublets Φ_1 and Φ_2 , after EWSB, in terms of their respective vacuum expectation values (VEVs) v_1 and v_2 , the Goldstone bosons G and G^\pm and the physical Higgs states as

$$\begin{aligned} \Phi_1 = & \frac{1}{\sqrt{2}} \begin{pmatrix} \sqrt{2}(G^+ c_\beta - H^+ s_\beta) \\ v_1 - h s_\alpha + H c_\alpha + i(G c_\beta - A s_\beta) \end{pmatrix}, \\ \Phi_2 = & \frac{1}{\sqrt{2}} \begin{pmatrix} \sqrt{2}(G^+ s_\beta + H^+ c_\beta) \\ v_2 + h c_\alpha + H s_\alpha + i(G s_\beta + A c_\beta) \end{pmatrix}, \end{aligned} \quad (2)$$

where $\beta \equiv \tan^{-1}(v_2/v_1)$ and α are the angles rotating the CP -odd and the CP -even interaction states, respectively,

into physical Higgs states, with s_x (c_x) implying $\sin(x)$ [$\cos(x)$]. Using the tadpole conditions of the \mathcal{V} , m_{11}^2 and m_{22}^2 can be replaced by v_1 and v_2 (and, subsequently, by t_β —short for $\tan \beta$ —and $v \equiv \sqrt{v_1^2 + v_2^2} = 246 \text{ GeV}$) as the free parameters of the model. Furthermore, the physical Higgs boson masses and the parameter $s_{\beta-\alpha}$ can be traded in for λ_{1-5} .

Multi- A production and benchmark scenarios: The benefit of using the physical Higgs boson masses as input parameters is that we can fix $m_h = 125 \text{ GeV}$, so that our analysis corresponds to the “standard hierarchy” scenario with $h = H_{\text{obs}}$ and a heavier H . For this scenario, our previous study [33] found that not only can the cross section for the EW production of the HA pair be up to 2 orders of magnitude larger than the gg/bb -induced one, but it also remains quite substantial for the subsequent states AAA and AAZ . Evidently, this cross section is more pronounced in parameter space regions where the H is produced on-shell, with a mass just above the AA or AZ decay threshold and a maximal corresponding branching ratio (BR). The requirement of the couplings of the h to be SM-like, as is the case for the H_{obs} , pushes the model into the so-called alignment limit, where $s_{\beta-\alpha} \rightarrow 1$ [35]. In this limit, the Hhh coupling is suppressed, unlike the HAA coupling. The HAZ coupling, which is proportional to $s_{\beta-\alpha}$, and hence the $\text{BR}(H \rightarrow AZ)$, is also naturally enhanced, while the $H \rightarrow VV$ decays, even when available, are suppressed.

In light of the above observations, our analysis pertains to a small m_A of 70 GeV . For such a light A , $b\bar{b}$ is by far the dominant decay mode and the multi-Higgs states that we are interested in here are thus the ones yielding at least $4b$ quarks via intermediate A s. Such states result from the EW production of either a neutral pair of Higgs bosons, both on-shell, as

$$\begin{aligned} AAA: & q\bar{q} \rightarrow H(\rightarrow AA)A \rightarrow 4b + X, \\ AAZ: & q\bar{q} \rightarrow H(\rightarrow AZ)A \rightarrow 4b + X, \\ AAWW: & q\bar{q} \rightarrow H^+(\rightarrow AW)H^-(\rightarrow AW) \rightarrow 4b + X, \end{aligned}$$

or a charged pair, as

$$\begin{aligned} AAW: & q\bar{q}' \rightarrow H^\pm(\rightarrow AW)A \rightarrow 4b + X, \\ AAAW: & q\bar{q}' \rightarrow H^\pm(H^\pm \rightarrow AW)H(\rightarrow AA) \rightarrow 4b + X, \\ AAZW: & q\bar{q}' \rightarrow H^\pm(H^\pm \rightarrow AW)H(\rightarrow AZ) \rightarrow 4b + X. \end{aligned}$$

Here the W and Z decay inclusively (i.e., both hadronically and leptonically) and X can thus be any additional quarks (including b quarks) and/or leptons.

In order to find model configurations with substantial EW production cross sections for a representative value of $m_A = 70 \text{ GeV}$, we numerically scanned the remaining parameters in the wide ranges

$$m_H: [2m_A - 250] \text{ GeV}, \quad m_{H^\pm}: [100-300] \text{ GeV},$$

$$s_{\beta-\alpha}: 0.9-1.0, \quad m_{12}^2: 0 - m_A^2 \sin\beta \cos\beta, \quad t_\beta: 1-60,$$

using the 2HDMC-1.8.0 code [36]. One of the most important constraints on the 2HDMs comes from the measurements of the oblique parameters S , T , and U , which in general forces m_{H^\pm} to lie close to m_H and/or m_A . The 2HDMC code internally calculates the theoretical predictions of these observables. In our scans, we required them to lie within the 95% confidence level (CL) ellipsoid based on the 2022 PDG values [37], $S = -0.01 \pm 0.07$ and $T = 0.04 \pm 0.06$, with correlations $\rho_{ST} = 0.92$ for $U = 0$. 2HDMC also checks each scanned point against theoretical constraints such as vacuum stability, tree-level unitarity, and perturbativity ($|\lambda_i| < 4\pi$). We moreover calculated the observable $\text{BR}(B \rightarrow X_s \gamma)$ using the SuperIso-v4.1 [38] program, and ensured that its prediction lied outside the exclusion contour in the $\{m_{H^\pm}, t_\beta\}$ plane derived in [34,39] based on experimental results.

Finally, we required all the Higgs states in each scanned point to satisfy the 95% CL constraints included in HiggsBounds-v5.10.2 [40]. We additionally made sure that the SM couplings of the h were consistent with the combined 2σ measurements for H_{obs} from the ATLAS and CMS Collaborations [41] using HiggsSignals-v2.6.2 [42-44]. From the successfully scanned parameter space points, we extracted a BP, for which the $\text{BR}(H \rightarrow AA)$ is almost 1 (and hence $\text{BR}(H \rightarrow AZ)$ is strongly suppressed). Some specifics of this BP are given in Table I.

Signal isolation.—The background events for the multi- b final states that we consider here originate predominantly from the QCD multijet and $t\bar{t}$ + jets processes. In our computation, we matched the multijet background up to four jets and the $t\bar{t}$ up to two jets. Our matched cross section for the multijet background in the 5-flavor scheme at the

TABLE I. Column 1: Input parameter values and $\text{BR}(H \rightarrow AA)$ for the BP (all masses are in GeV). Column 2: Cross section for each of the signal channels, assuming a next-to-next-to-leading order k factor of 1.35 [45]. Columns 3-5: Total signal and background cross sections after applying all the selection cuts, and the discovery significance for the three non-SM Higgs bosons.

Parameters	Preselection	Reconstructed Higgs		
	cross section (fb)	σ_S (fb)	σ_B (fb)	S/\sqrt{B}
$m_{H^\pm} = 169.7$	AAA: 171.6		A	
$m_H = 144.7$	AAZ: 0.76	15.4	8864	8.9σ
$t_\beta = 7.47$	AAWW: 25.2		H^\pm	
$s_{\beta-\alpha} = 0.99$	AAW: 142.3	2.22	482	5.5σ
$m_{12}^2 = 2355$	AAAW: 79.7		H	
$\text{BR}(AA) = 0.99$	AAZW: 0.35	2.55	309	7.9σ

LHC with $\sqrt{s} = 13$ TeV is 8.98×10^6 pb, with NNPDF23_lo_as_0130 [46] parton distribution functions (PDFs) and a matching scale of 67.5 GeV. The $t\bar{t}$ production cross section is 833.9 pb, as calculated with the Top++2.0 [47] program, assuming a top quark mass of 173.2 GeV. For our simulation we generated 2×10^8 multijet events and 10^7 $t\bar{t}$ events. Other possible background processes include $t\bar{t}b\bar{b}$, $t\bar{t} + V$ (where $V = Z/W$), $V + \text{jets}$, ZZ and hZ , but we found them to be negligible after the selections.

For our selected BP, we again used the NNPDF23_lo_as_0130 PDF set to estimate the multi- b signal events. We performed event-generation and parton shower with MadGraph5_aMC@NLO [48,49] and PYTHIA-8.2 [50,51], using the anti- k_t algorithm [52] with $R = 0.4$ for jet reconstruction. For b tagging, we used the p_T -dependent efficiencies corresponding to the ‘‘DeepCSV Medium’’ working point based on the $\sqrt{s} = 13$ TeV data from the CMS Collaboration [53]. We used Delphes-3.4.2 [54] for event generation, which was followed by analysis in the Root [55] framework. We retained the default CMS jet energy scale in Delphes. The primary selection cuts we applied for signal isolation include: $p_T > 20$ GeV and $|\eta| < 2.5$ for all the jets in any reconstructed object. Further selections that we made for each Higgs state are explained below.

Reconstruction of the A : (1) Since all the signal processes contain at least two A ’s, the events should contain at least 4 b jets, a , b , c , and d , which can be resolved into pairs 1 and 2. For this purpose we used a pairing algorithm for the leading b jets to choose one combination out of the possible three: $(a, b; c, d)$, $(a, c; b, d)$, and $(a, d; b, c)$, which minimizes [56]

$$\Delta R = |(\Delta R_1 - 0.8)| + |(\Delta R_2 - 0.8)|. \quad (3)$$

Here, for a given combination,

$$\Delta R_1 = \sqrt{(\eta_a - \eta_b)^2 + (\phi_a - \phi_b)^2},$$

$$\Delta R_2 = \sqrt{(\eta_c - \eta_d)^2 + (\phi_c - \phi_d)^2}, \quad (4)$$

and offsetting each of these by 0.8 omits the b -jet pairings with too large an overlap in the $\{\eta, \phi\}$ space. This algorithm is motivated by the idea that the b jets coming from a resonance (presumably the A) are closer together compared to the uncorrelated ones. (2) After the pairing, we imposed an asymmetry cut,

$$\bar{\alpha} = \frac{|m_1 - m_2|}{m_1 + m_2} < 0.2, \quad (5)$$

where m_1 and m_2 are the invariant masses of the two b -jet pairs. This cut ensures that these two pairs are from identical resonances, i.e., from AA .

Reconstruction of the H^\pm : (1) All events should contain at least 4 b -tagged jets and a pair of leading jets (thus corresponding to the dominant $q\bar{q}' \rightarrow A_1 H^\pm \rightarrow A_1 A_2 W^\pm \rightarrow 4b + jj$ process). (2) The invariant mass of the leading jj should lie within the $m_W \pm 25$ GeV mass window. (3) The four b jets were combined into two b -jet pairs and only events where the invariant mass of each of these pairs lied within a 45 GeV window around m_A and satisfied the asymmetry cut $\bar{\alpha} < 0.2$ were selected. This criterion reduces the background significantly. The vector p_T sum of the b -jet pairs estimated the p_T of the reconstructed A 's, which are identified as A_1 and A_2 such that $p_T(A_1) > p_T(A_2)$ (since A_2 originates from the H^\pm decay and is softer). (4) We calculated the invariant mass of the $2b + jj$ system, where “ $2b$ ” is the softer pair (identified as the A_2), to obtain the m_{H^\pm} . (5) When more than one pairings of the b jets satisfy the above condition, we selected the combination which maximized the separation $\Delta R = \sqrt{(\Delta\eta)^2 + (\Delta\phi)^2}$ of the reconstructed H^\pm and A_1 .

Reconstruction of the H : (1) The dominant signal process is $q\bar{q} \rightarrow A_1 H \rightarrow A_1 A_2 A_3 \rightarrow 4b + X$, so each event should contain at least six b -tagged jets. We combined these into three b -jet pairs and selected the combination for which the invariant mass of each pair lied within a 45 GeV window around m_A , and also satisfied the $\bar{\alpha}$ cut. (We note here that the reconstruction efficiency for all the Higgs bosons can be further improved by imposing $\bar{\alpha} < 0.1$ and some other selection criteria used in [56]. However, due to the large cross section of the QCD background, simulating it for such a strong selection cut would require much more substantial computational resources.) (2) The p_T of each b -jet pair was obtained by summing the 4-momenta of the two b jets in it. Out of the three pairs, we identified the one with the highest p_T as the prompt A_1 . The remaining system of 4 b jets then corresponded to the $A_2 A_3$ pair from H decay, and its invariant mass thus reconstructed the m_H . (3) As in the case of the H^\pm , if multiple pairings of the b jets satisfied the above criteria, we used that $4b$ -jet system for reconstructing the H which maximized its separation from the third b -jet pair (i.e., the prompt A_1) in the $\{\eta, \phi\}$ space. (4) Since tagging 6 b jets is highly challenging due to finite (mis-)tagging, events with at least 5 b jets were also used for reconstructing the H . In this case, the light jet with the leading p_T was first assumed to be the 6th b jet for performing steps 1–3. If this jet failed to satisfy the pairing criteria above, these steps were repeated sequentially for the jet with the next highest p_T , until the correct jet was found.

Significances at the LHC.—Using the steps detailed in the previous section, we calculated the signal (background) event rates, S (B) assuming an integrated luminosity of 3000 fb^{-1} at the LHC for our BP. In Fig. 1 we show the normalized invariant mass distributions of the b -jet pairs for these events. The subscript a implies the distribution for the pair containing the leading b jet. The signal distributions in

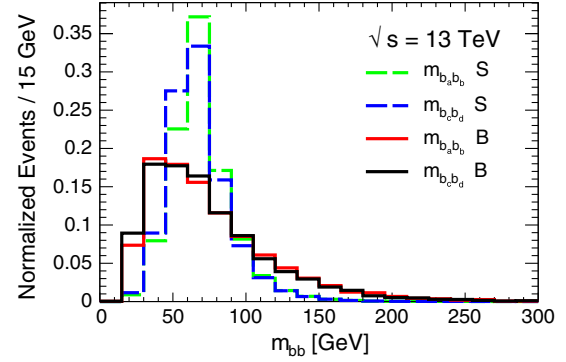


FIG. 1. m_{bb} distributions for the signal (green and blue, dashed) and background (red and black, solid) events for the BP.

this figure as well as the subsequent figures include all the signal modes mentioned in Sec. II, while the background distributions include both multi-jet and $t\bar{t} + \text{jets}$. Clearly, the invariant masses peak at the true m_A . Figure 2 similarly shows the distributions of the $bbjj$ invariant mass, which peaks around the true $m_{H^\pm} = 169.7$ GeV.

Fig. 3 depicts the reconstruction of the H , as described in Sec. III. The red-dashed signal histogram, corresponding to events with at least 5 b jets, has a peak around the true $m_H = 144.7$ GeV. In this figure, the blue-dotted histogram shows the invariant mass distribution when events with 6 b -tagged jets are considered, which results in a better mass reconstruction compared to events with 5 b jets. However, as noted earlier, estimation of the background for events with 6 b jets is beyond the reach of our analysis.

From these histograms, we chose three bins around the mass of each of the non-SM Higgs boson to estimate the statistical significance, S/\sqrt{B} of its signature. For the reconstruction of the A , the S (B) implies the mean of the number of events in the bins covering m_{bb} from 45 to 90 GeV for the two signal (background) distributions in Fig. 1.

These significances are shown in Table I. The highest significance was obtained for the A , since all the signal modes contribute to its reconstruction. In the case of the H^\pm

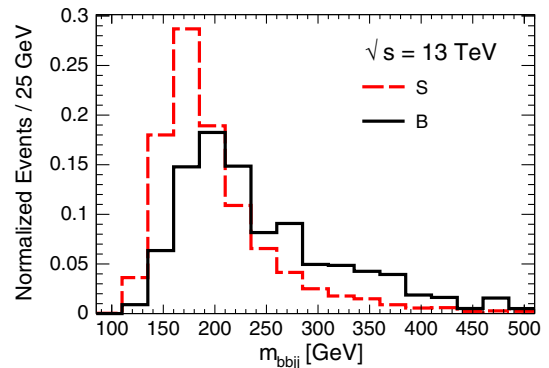


FIG. 2. m_{bbjj} distributions for the signal (red, dashed) and background (black, solid) events for the BP.

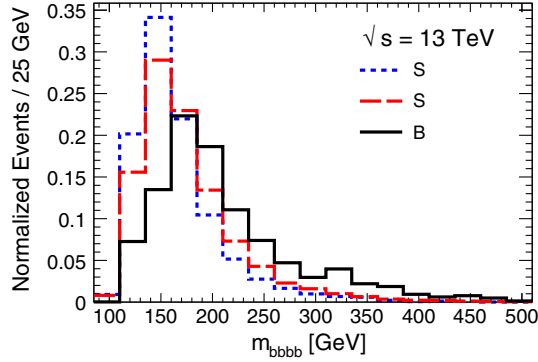


FIG. 3. m_{bbbb} distributions for the signal (red and blue, dashed) and background (black, solid) events for the BP.

and H instead, the reconstruction algorithms are based on the signal topologies AAW and AAA , respectively, and the other contributions thus get diminished. For the H , the requirement of at least 5 b -tagged jets strongly suppresses the QCD background compared to the signal within the three relevant invariant mass bins, which leads to a considerably higher S/\sqrt{B} for it compared to the H^\pm , as seen in the table. We point out again that, for the H signal, this significance has been calculated for 5 b -tagged jets and one light jet (rather than for 6 b jets).

Conclusions.—In a new physics framework containing multiple Higgs fields, such as the 2HDM studied here, a full reconstruction of the Higgs potential would entail observing all the additional physical Higgs states and measuring their masses and couplings. Numerous attempts, both theoretical and experimental ones, have been made to extract signatures of the two neutral Higgs bosons, besides the SM-like one, as well as the charged scalar in various Types of the 2HDM. These studies, however, generally focus on a QCD-induced single- or multiple-production, followed by a specific decay channel, of any one of these additional states, for investigating its discovery prospects at the LHC.

In this Letter we have shown, for the very first time, that all the three non-SM Higgs bosons in this model might be detectable in the unique final state with 4 (or more) b jets at the HL-LHC. This is possible for specific (and rather narrow) parameter space configurations, wherein intermediate pairs of relatively light Higgs bosons, produced on-shell, lead to multi- A states, which subsequently decay in the $b\bar{b}$ channel. Our sophisticated MC analysis yielded a $S/\sqrt{B} > 5\sigma$ for the signals of all the three non-SM Higgs states.

We therefore strongly advocate systematic investigations of the EW-induced processes alongside the time-honored QCD-initiated ones, as they may prove crucial for nailing

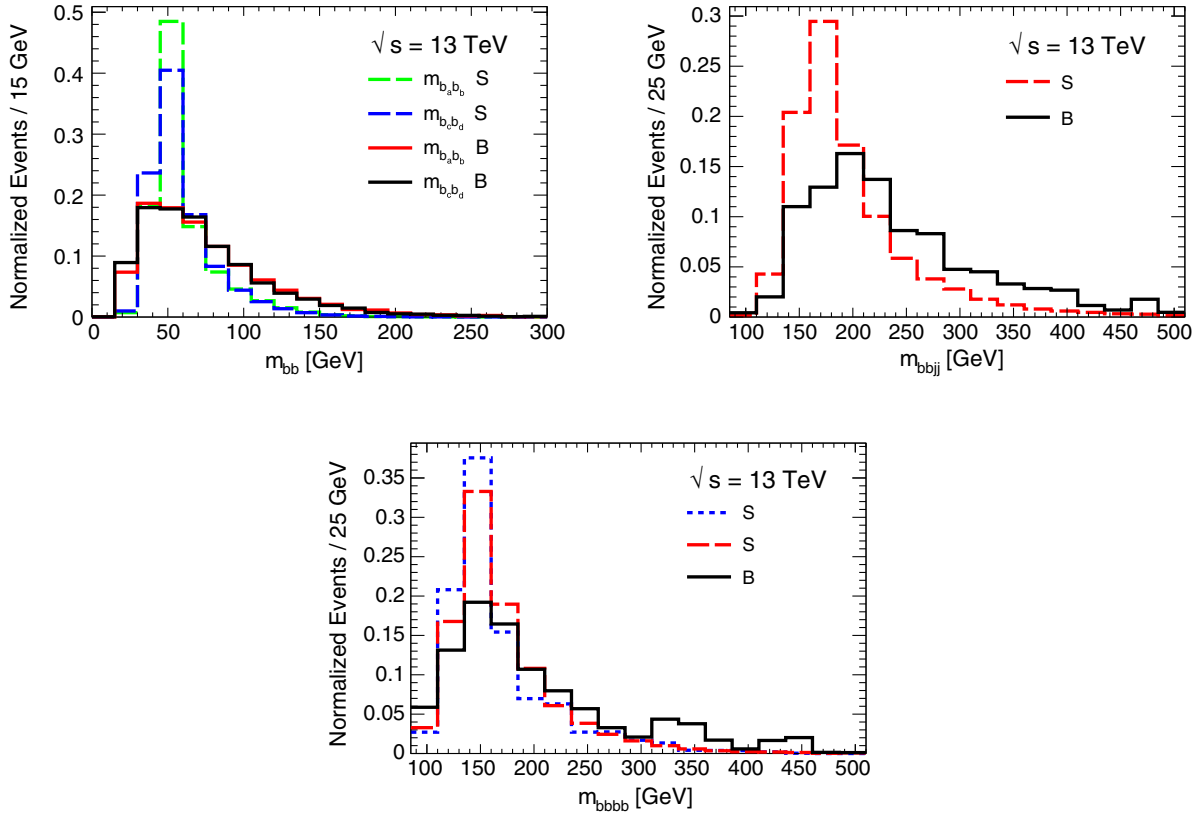


FIG. 4. Normalized invariant mass distributions for the BP'. Top-left: m_{bb} for the signal (green and blue, dashed) and background (red and black, solid) events. Top-right: m_{bbjj} for the signal (red, dashed) and background (black, solid) events. Bottom: m_{bbbb} for the signal (red and blue, dashed) and background (black, solid).

TABLE II. Input parameters, signal and background cross sections, and discovery significances for the three non-SM Higgs bosons of the BP'.

Parameters	Preselection	Reconstructed Higgs		
	cross section (fb)	σ_S (fb)	σ_B (fb)	S/\sqrt{B}
$m_{H^\pm} = 169.8$	AAA: 101.3		A	
$m_H = 150.0$	AAZ: 79.3	10.4	10175	5.7σ
$t_\beta = 17.1$	AAWW: 27.7		H^\pm	
$s_{\beta-\alpha} = 0.98$	AAW: 198.0	1.33	491	3.3σ
$m_{12}^2 = 1275$	AAAW: 37.1		H	
$\text{BR}(AA) = 0.48$	AAZW: 29.0	1.06	256	3.6σ

down the Type-I 2HDM as (the low-energy limit of) the new physics framework prevalent in nature.

S. Mo. is supported in part through the NExT Institute and the STFC Consolidated Grant No. ST/L000296/1. P. S. is supported by the National Research Foundation of Korea, Grant No. NRF-2022R1A2C1007583. T. M.'s work is supported by JSPS KAKENHI Grant No. 22F21324. The authors would also like to thank the KIAS Center for Advanced Computation for providing computing resources.

Appendix: A lighter A.—In order to test the efficiency of our reconstruction method for the scenario with substantial partial width of the decay of the H into AZ , we picked a BP', for which $\text{BR}(H \rightarrow AZ) = 0.5$ and $m_A = 50$ GeV. m_H and m_{H^\pm} for this BP' are almost identical to the respective ones for our main BP, and it therefore allows us to assess the impact of also a smaller m_A , besides a significantly reduced $\text{BR}(H \rightarrow AA)$, on our analysis. The invariant mass distributions for the BP' are shown in Fig. 4 for the A (top-left), H^\pm (top-right), and H (bottom), and closely resemble the respective ones for the $m_A = 70$ GeV BP.

For the BP', we see relatively low significances for all the Higgs bosons in Table II. Our reconstruction algorithm for the H is thus much more efficient when its decay to AA is highly dominant. Furthermore, a lighter A results in much softer b jets, which lowers the selection efficiency overall. Despite all these deficiencies, the signal significances are still a formidable $> 3\sigma$ for all the Higgs bosons for this BP', thus demonstrating the strength of our proposed reconstruction method.

*tanmoy@het.phys.sci.osaka-u.ac.jp

†s.moretti@soton.ac.uk, stefano.moretti@physics.uu.se

‡munir1@stolaf.edu

§prasenjit.sanyal01@gmail.com

[1] Georges Aad *et al.* (ATLAS Collaboration), Observation of a new particle in the search for the Standard Model Higgs boson with the ATLAS detector at the LHC, *Phys. Lett. B* **716**, 1 (2012).

- [2] Serguei Chatrchyan *et al.* (CMS Collaboration), Observation of a new boson at a mass of 125 GeV with the CMS experiment at the LHC, *Phys. Lett. B* **716**, 30 (2012).
- [3] Sheldon L. Glashow and Steven Weinberg, Natural conservation laws for neutral currents, *Phys. Rev. D* **15**, 1958 (1977).
- [4] E. A. Paschos, Diagonal neutral currents, *Phys. Rev. D* **15**, 1966 (1977).
- [5] John F. Gunion, Howard E. Haber, Gordon L. Kane, and Sally Dawson, The Higgs Hunter's Guide, *Front. Phys.* **80**, 1 (2000), <https://inspirehep.net/literature/279039>.
- [6] G. C. Branco, P. M. Ferreira, L. Lavoura, M. N. Rebelo, Marc Sher, and J. P. Silva, Theory and phenomenology of two-Higgs-doublet models, *Phys. Rep.* **516**, 1 (2012).
- [7] Abdesslam Arhrib, Rachid Benbrik, Chuan-Hung Chen, Renato Guedes, and Rui Santos, Double Neutral Higgs production in the Two-Higgs doublet model at the LHC, *J. High Energy Phys.* **08** (2009) 035.
- [8] Benoit Hespel, David Lopez-Val, and Eleni Vryonidou, Higgs pair production via gluon fusion in the Two-Higgs-Doublet Model, *J. High Energy Phys.* **09** (2014) 124.
- [9] Rikard Enberg, William Klemm, Stefano Moretti, and Shoaib Munir, Electroweak production of light scalar-pseudoscalar pairs from extended Higgs sectors, *Phys. Lett. B* **764**, 121 (2017).
- [10] Abdesslam Arhrib, Rachid Benbrik, and Stefano Moretti, Bosonic decays of charged Higgs bosons in a 2HDM type-I, *Eur. Phys. J. C* **77**, 621 (2017).
- [11] Abdesslam Arhrib, Rachid Benbrik, Stefano Moretti, Abdessamad Rouchad, Qi-Shu Yan, and Xianhui Zhang, Multi-photon production in the Type-I 2HDM, *J. High Energy Phys.* **07** (2018) 007.
- [12] Abdesslam Arhrib, Rachid Benbrik, Rikard Enberg, William Klemm, Stefano Moretti, and Shoaib Munir, Identifying a light charged Higgs boson at the LHC Run II, *Phys. Lett. B* **774**, 591 (2017).
- [13] Wenhai Xie, R. Benbrik, Abdeljalil Habjia, Souad Taj, Bin Gong, and Qi-Shu Yan, Signature of 2HDM at Higgs factories, *Phys. Rev. D* **103**, 095030 (2021).
- [14] Abdesslam Arhrib, Rachid Benbrik, Hicham Harouiz, Stefano Moretti, Yan Wang, and Qi-Shu Yan, Implications of a light charged Higgs boson at the LHC run III in the 2HDM, *Phys. Rev. D* **102**, 115040 (2020).
- [15] A. Arhrib, R. Benbrik, M. Krab, B. Manaut, S. Moretti, Yan Wang, and Qi-Shu Yan, New discovery modes for a light charged Higgs boson at the LHC, *J. High Energy Phys.* **10** (2021) 073.
- [16] Yan Wang, A. Arhrib, R. Benbrik, M. Krab, B. Manaut, S. Moretti, and Qi-Shu Yan, Analysis of $W + 4\gamma$ in the 2HDM Type-I at the LHC, *J. High Energy Phys.* **12** (2021) 021.
- [17] Oliver Atkinson, Matthew Black, Alexander Lenz, Aleksey Rusov, and James Wynne, Cornering the two Higgs doublet model Type II, *J. High Energy Phys.* **04** (2022) 172.
- [18] Tanmoy Mondal and Prasenjit Sanyal, Same sign trilepton as signature of charged Higgs in two Higgs doublet model, *J. High Energy Phys.* **05** (2022) 040.
- [19] Shinya Kanemura, Michihisa Takeuchi, and Kei Yagyu, Probing double-aligned two-Higgs-doublet models at the LHC, *Phys. Rev. D* **105**, 115001 (2022).

- [20] M. Krab, M. Ouchemhou, A. Arhrib, R. Benbrik, B. Manaut, and Qi-Shu Yan, Single charged Higgs boson production at the LHC, *Phys. Lett. B* **839**, 137705 (2023).
- [21] Kingman Cheung, Adil Jueid, Jinheung Kim, Soojin Lee, Chih-Ting Lu, and Jeonghyeon Song, Comprehensive study of the light charged Higgs boson in the type-I two-Higgs-doublet model, *Phys. Rev. D* **105**, 095044 (2022).
- [22] Jinheung Kim, Soojin Lee, Jeonghyeon Song, and Prasenjit Sanyal, Fermiophobic light Higgs boson in the type-I two-Higgs-doublet model, *Phys. Lett. B* **834**, 137406 (2022).
- [23] Jinheung Kim, Soojin Lee, Prasenjit Sanyal, Jeonghyeon Song, and Daohan Wang, $\tau^\pm\nu\gamma\gamma$ and $\ell^\pm\ell^\pm\gamma\gamma\cancel{E}_T X$ to probe the fermiophobic Higgs boson with high cutoff scales, *J. High Energy Phys.* **04** (2023) 083.
- [24] Yi-Lun Chung, Kingman Cheung, and Shih-Chieh Hsu, Sensitivity of two-Higgs-doublet models on Higgs-pair production via $bb\text{-}bb$ final state, *Phys. Rev. D* **106**, 095015 (2022).
- [25] Anna Ivina (ATLAS Collaboration), Search for light charged Higgs boson in $t \rightarrow H^\pm + b(H^\pm \rightarrow cb)$ decays with the ATLAS detector at LHC, *Proc. Sci., EPS-HEP2021* (2022) 631.
- [26] G. Aad *et al.* (ATLAS Collaboration), Search for heavy resonances decaying into a Z or W boson and a Higgs boson in final states with leptons and b-jets in 139 fb^{-1} of pp collisions at $\sqrt{s} = 13\text{ TeV}$ with the ATLAS detector, *J. High Energy Phys.* **06** (2023) 016.
- [27] ATLAS Collaboration, Search for displaced photons produced in exotic decays of the Higgs boson using 13 TeV pp collisions with the ATLAS detector, *Phys. Rev. D* **108**, 032016 (2023).
- [28] G. Aad *et al.* (ATLAS Collaboration), A search for heavy Higgs bosons decaying into vector bosons in same-sign two-lepton final states in pp collisions at $\sqrt{s} = 13\text{ TeV}$ with the ATLAS detector, *J. High Energy Phys.* **07** (2023) 200.
- [29] Armen Tumasyan *et al.* (CMS Collaboration), Search for new particles in an extended Higgs sector with four b quarks in the final state at $s = 13\text{ TeV}$, *Phys. Lett. B* **835**, 137566 (2022).
- [30] CMS Collaboration, Search for a massive scalar resonance decaying to a light scalar and a Higgs boson in the four b quarks final state with boosted topology, *Phys. Lett. B* **842**, 137392 (2022).
- [31] CMS Collaboration, Search for a charged Higgs boson decaying into a heavy neutral Higgs boson and a W boson in proton-proton collisions at $\sqrt{s} = 13\text{ TeV}$, *J. High Energy Phys.* **09** (2023) 032.
- [32] CMS Collaboration, Search for the exotic decay of the Higgs boson into two light pseudoscalars with four photons in the final state in proton-proton collisions at $\sqrt{s} = 13\text{ TeV}$, *J. High Energy Phys.* **07** (2023) 148.
- [33] Rikard Enberg, William Klemm, Stefano Moretti, and Shoaib Munir, Electroweak production of multiple (pseudo)scalars in the 2HDM, *Eur. Phys. J. C* **79**, 512 (2019).
- [34] Farvah Mahmoudi, Overview of the interpretation of indirect searches for charged Higgs bosons in the 2HDM, *Proc. Sci., CHARGED2016* (2017) 012.
- [35] Jérémy Bernon, John F. Gunion, Howard E. Haber, Yun Jiang, and Sabine Kraml, Scrutinizing the alignment limit in two-Higgs-doublet models. II. $m_H = 125\text{ GeV}$, *Phys. Rev. D* **93**, 035027 (2016).
- [36] David Eriksson, Johan Rathsman, and Oscar Stal, 2HDMC: Two-Higgs-doublet model calculator physics and manual, *Comput. Phys. Commun.* **181**, 189 (2010).
- [37] R. L. Workman *et al.* (Particle Data Group Collaboration), Review of particle physics, *Prog. Theor. Exp. Phys.* **2022**, 083C01 (2022).
- [38] F. Mahmoudi, SuperIso v2.3: A program for calculating flavor physics observables in Supersymmetry, *Comput. Phys. Commun.* **180**, 1579 (2009).
- [39] Prasenjit Sanyal, Limits on the charged Higgs parameters in the two Higgs doublet model using CMS $\sqrt{s} = 13\text{ TeV}$ results, *Eur. Phys. J. C* **79**, 913 (2019).
- [40] Philip Bechtle, Oliver Brein, Sven Heinemeyer, Oscar Stål, Tim Stefaniak, Georg Weiglein, and Karina E. Williams, HiggsBounds-4: Improved tests of extended Higgs sectors against exclusion bounds from LEP, the tevatron and the LHC, *Eur. Phys. J. C* **74**, 2693 (2014).
- [41] Jonathon Mark Langford (ATLAS, CMS Collaborations), Combination of Higgs measurements from ATLAS and CMS: Couplings and \cancel{E}_T framework, *Proc. Sci., LHCP2020* (2021) 136.
- [42] Philip Bechtle, Sven Heinemeyer, Oscar Stål, Tim Stefaniak, and Georg Weiglein, HiggsSignals: Confronting arbitrary Higgs sectors with measurements at the Tevatron and the LHC, *Eur. Phys. J. C* **74**, 2711 (2014).
- [43] Philip Bechtle, Sven Heinemeyer, Tobias Klingl, Tim Stefaniak, Georg Weiglein, and Jonas Wittbrodt, HiggsSignals-2: Probing new physics with precision Higgs measurements in the LHC 13 TeV era, *Eur. Phys. J. C* **81**, 145 (2021).
- [44] Henning Bahl, Thomas Biekötter, Sven Heinemeyer, Cheng Li, Steven Paasch, Georg Weiglein, and Jonas Wittbrodt, HiggsTools: BSM scalar phenomenology with new versions of HiggsBounds and HiggsSignals, *Comput. Phys. Commun.* **291**, 108803 (2023).
- [45] Henning Bahl, Tim Stefaniak, and Jonas Wittbrodt, The forgotten channels: Charged Higgs boson decays to a W and a non-SM-like Higgs boson, *J. High Energy Phys.* **06** (2021) 183.
- [46] Richard D. Ball *et al.* (NNPDF Collaboration), Parton distributions from high-precision collider data, *Eur. Phys. J. C* **77**, 663 (2017).
- [47] Michal Czakon and Alexander Mitov, Top++: A program for the calculation of the top-pair cross-section at hadron colliders, *Comput. Phys. Commun.* **185**, 2930 (2014).
- [48] Johan Alwall, Michel Herquet, Fabio Maltoni, Olivier Mattelaer, and Tim Stelzer, MadGraph 5: Going beyond, *J. High Energy Phys.* **06** (2011) 128.
- [49] J. Alwall, R. Frederix, S. Frixione, V. Hirschi, F. Maltoni, O. Mattelaer, H. S. Shao, T. Stelzer, P. Torrielli, and M. Zaro, The automated computation of tree-level and next-to-leading order differential cross sections, and their matching to parton shower simulations, *J. High Energy Phys.* **07** (2014) 079.
- [50] Torbjorn Sjostrand, Stephen Mrenna, and Peter Z. Skands, PYTHIA6.4 Physics and Manual, *J. High Energy Phys.* **05** (2006) 026.

- [51] Torbjörn Sjöstrand, Stefan Ask, Jesper R. Christiansen, Richard Corke, Nishita Desai, Philip Ilten, Stephen Mrenna, Stefan Prestel, Christine O. Rasmussen, and Peter Z. Skands, An Introduction to PYTHIA8.2, *Comput. Phys. Commun.* **191**, 159 (2015).
- [52] Matteo Cacciari, Gavin P. Salam, and Gregory Soyez, The Anti-k(t) jet clustering algorithm, *J. High Energy Phys.* **04** (2008) 063.
- [53] A. M. Sirunyan *et al.* (CMS Collaboration), Identification of heavy-flavour jets with the CMS detector in pp collisions at 13 TeV, *J. Instrum.* **13**, P05011 (2018).
- [54] J. de Favereau, C. Delaere, P. Demin, A. Giammanco, V. Lemaître, A. Mertens, and M. Selvaggi (DELPHES 3 Collaboration), DELPHES 3, A modular framework for fast simulation of a generic collider experiment, *J. High Energy Phys.* **02** (2014) 057.
- [55] R. Brun and F. Rademakers, ROOT: An object oriented data analysis framework, *Nucl. Instrum. Methods Phys. Res., Sect. A* **389**, 81 (1997).
- [56] CMS Collaboration, Search for resonant and nonresonant production of pairs of dijet resonances in proton-proton collisions at $\sqrt{s} = 13$ TeV, *J. High Energy Phys.* **07** (2023) 161.